Beta decay of $^{27-32}$Na and their descendants

C. Détraz, D. Guillemaud, G. Huber, R. Klapisch, M. Langevin, F. Naulin, C. Thibault, L.C. Carraz,* and F. Touchard

Laboratoire René Bernas, Centre de Spectrométrie Nucléaire et de Spectrométrie de Masse, 91406 Orsay, France and Institut de Physique Nucléaire, 91406 Orsay, France

(Received 10 July 1978)

The γ activities from the β decay of Na isotopes up to ^{32}Na, which are formed in high-energy fragmentation and analyzed through mass spectrometry techniques, are observed, as well as those from their Mg or Al descendants. Their intensities are measured, in most cases, in absolute value. The radioactive half-lives of ^{29}Mg, ^{30}Mg, and ^{31}Mg are determined. Delayed-neutron branching ratios P_n are measured for ^{29}Na, ^{30}Na, and ^{32}Na. In some cases, partial branching ratios to excited states of the daughter nucleus are also measured. The most prominent γ ray in the β decay of even Na isotopes is assigned to $2^+ \rightarrow 0^+$ transition in the daughter Mg isotopes. The position of the first excited 2^+ level is therefore deduced for ^{30}Mg and ^{32}Mg. For ^{32}Mg, the excitation energy drops markedly. It is taken as an indication of a stronger deformation for that isotope.

[RADIOACTIVITY $^{27-32}$Na, $^{29-31}$Mg, ^{31}Al; measured $T_{1/2}$, E_γ, $\beta\gamma$ coin; deduced I_γ, I_β, P_n.]

I. INTRODUCTION

There is an increasing interest in nuclei far from the valley of β stability, with a Z/N ratio very different from the value corresponding to the well studied β stable or near to β stable isotopes. The study of such exotic nuclei is expected to shed a new light onto the properties of nuclear systems.

A few years ago, a measurement of the mass excesses of very neutron-rich Na isotopes[1] showed a marked discontinuity for the two-neutron binding energy of these isotopes at $N=19$. This has been interpreted as due to the onset of a large deformation for the Na ground states. Hartree-Fock calculations support this interpretation.[2] Hence $N=20$, which corresponds to the closure of the $(1d, 2s)$ shell for less exotic nuclei, would be located in a region of large deformation far from the valley of stability.

It has long been recognized that the magic numbers observed for the stable or nearly stable nuclei, which are well accounted for by a spherical harmonic oscillator, do not necessarily hold for very different nuclei. In the particular case of Na isotopes, the Hartree-Fock calculation mentioned above[2] is a first example. Two other theoretical results point in the same direction. First, Sheline[3] has shown that the $N=20$ magic number disappears for an asymmetric rotor, and that new magic numbers are found, such as 14 and 26 for oblate nuclei ($\epsilon=-0.75$), and 10 and 16 for prolate nuclei ($\epsilon=+0.6$). Second, even for spherical nuclei, a large neutron excess also produces a change in magic numbers. A self-consistent calculation by the energy-density formalism[4] finds magic numbers at $N=16$ and 34 for Na isotopes. All these calculations would indeed predict that $N=20$, far from being a magic number, could correspond to a new region of deformation.

The observation of the decay modes of the exotic Na isotopes was undertaken to examine this problem since the location of energy levels in the daughter Mg isotopes can provide a direct, if not unambiguous, evidence for a deformation of these nuclei. The large cross sections observed for high-energy fragmentation of heavy nuclei, together

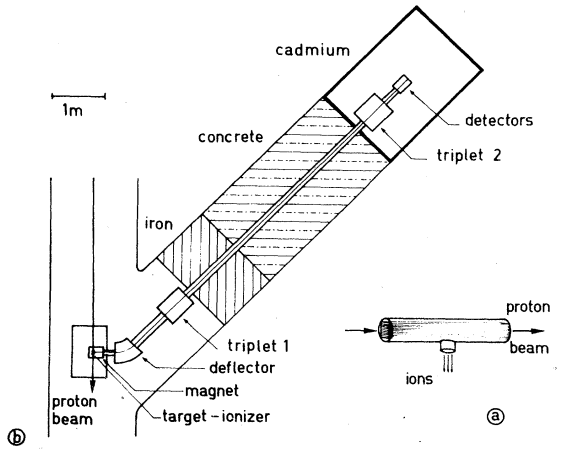

FIG. 1. Schematic view of the experimental setup. (a) Detail of the target ionizer. The graphite foils covered with uranium are in a tantalum oven. The alkali atoms which diffuse out, are ionized in the exhaust tubing made of rhenium. (b) Schematic view of the experimental setup in the fast extracted beam of 24 GeV protons produced by the CERN synchrotron.

 © 1979 The American Physical Society

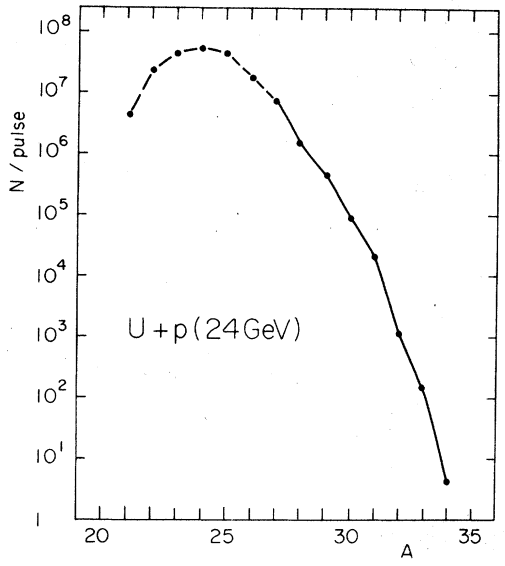

FIG. 2. Number of Na ions collected on the Al foil in the counting area for 10^{13} protons per pulse.

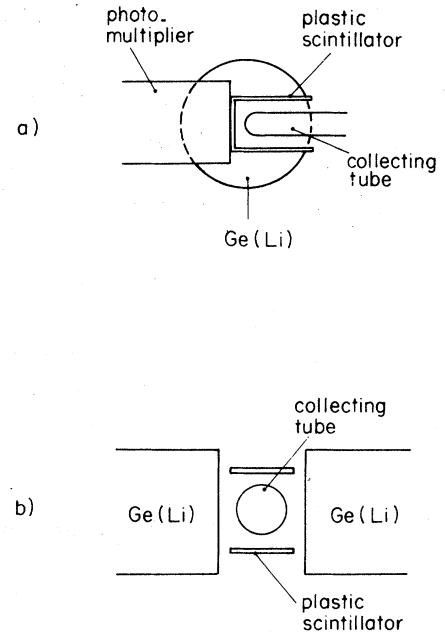

FIG. 3. Sketch of the geometrical arrangement of the detectors of β rays (plastic scintillator) and γ rays [two Ge(Li) detectors].

with the selectivity and efficiency of the mass spectrometry method, allow for the production of large numbers of very neutron-rich isotopes, hence for the use of the classical tools of nuclear spectroscopy.

Four years ago,[5] some results on the β decay of $^{27-31}$Na isotopes produced by the same method were already obtained. The delayed neutron branching ratios and the radioactive half-lives were reported. Some γ activities were observed and measured. Since then, the intensity of the CERN proton synchrotron and the efficiency of the mass

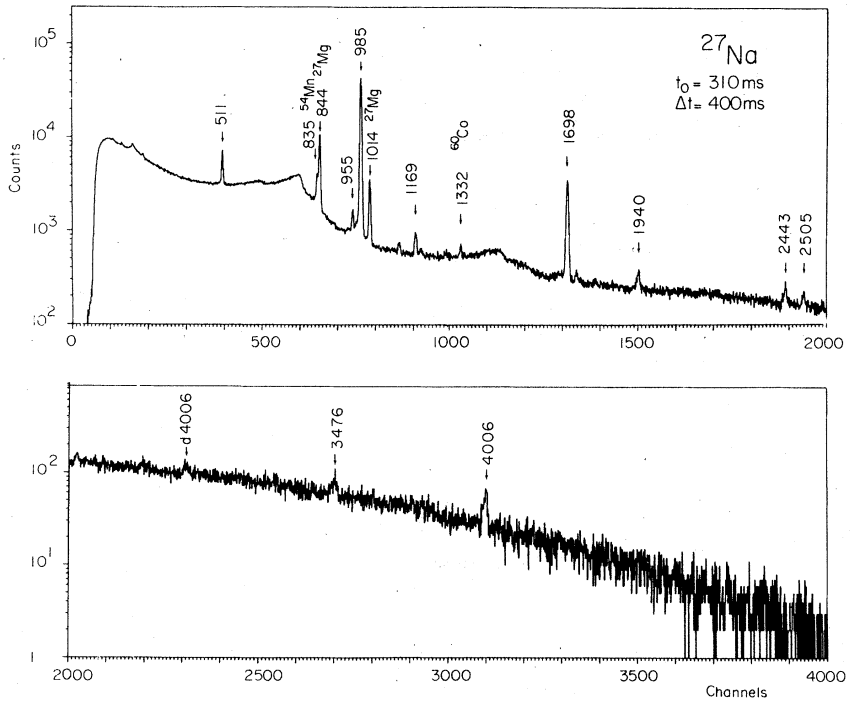

FIG. 4. Energy spectrum of the γ rays observed in the β decay of ^{27}Na collected from the time t_0 after the beam burst and during a measuring time Δt. The γ rays from the decay of ^{27}Na are labeled by their energies (keV). Simple and double escape peaks are labeled by their energies and the emitting nucleus.

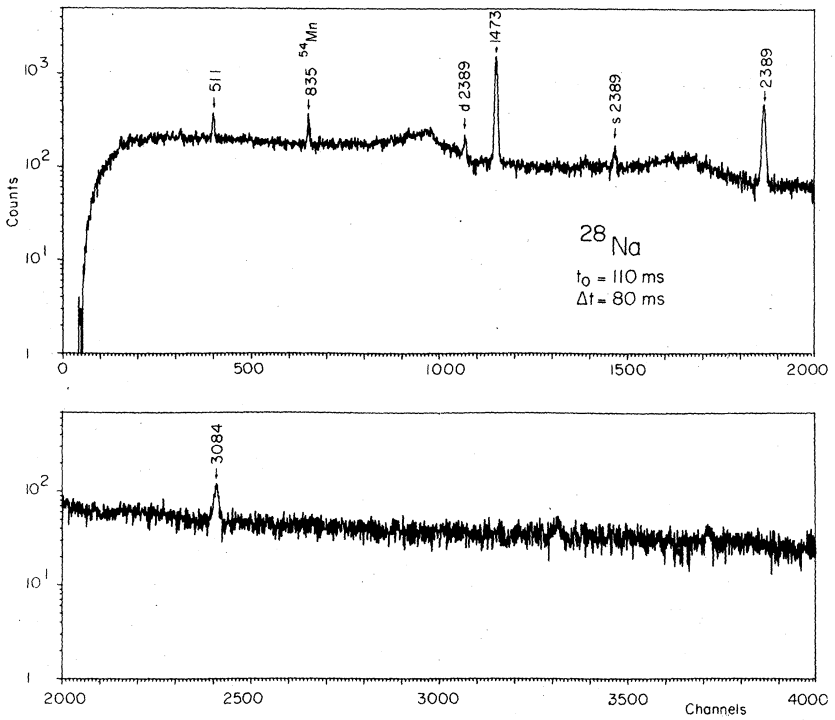

FIG. 5. Energy spectrum of the γ rays observed in the β decay of ^{28}Na (see Fig. 4).

spectrometer have been increased by factors of about 10 and 20, respectively. These improvements, together with a better shielding, result in a more sensitive and accurate experiment.

In this paper we report on the β-decay properties (γ activities, half-lives, delayed neutron emission, β branching ratios) of the exotic Na isotopes up to ^{32}Na and their descendants. Similar

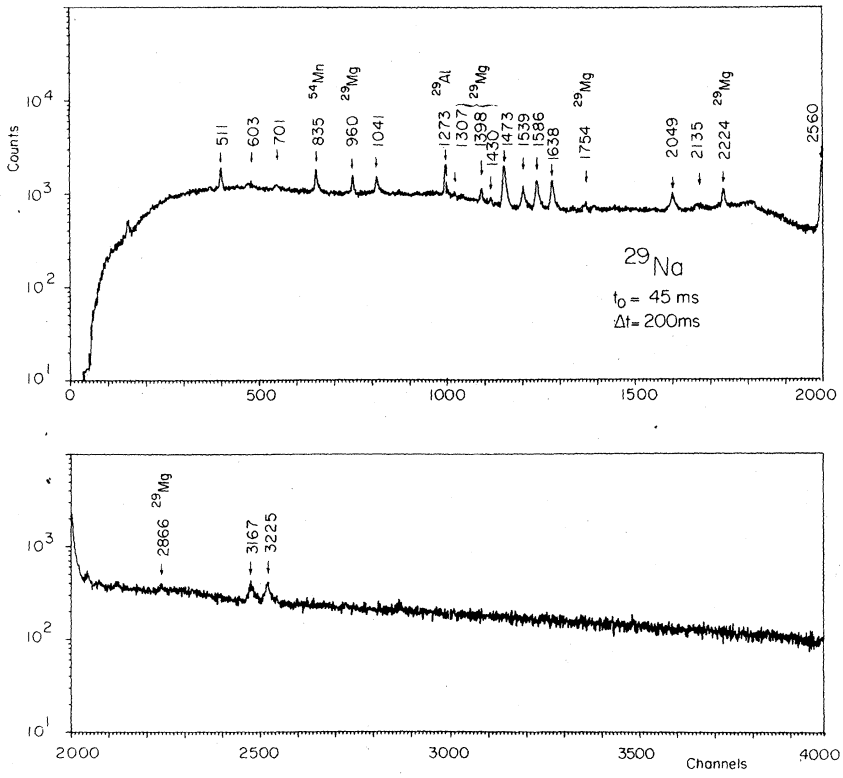

FIG. 6. Energy spectrum of the γ rays observed in the β decay of ^{29}Na (see Fig. 4).

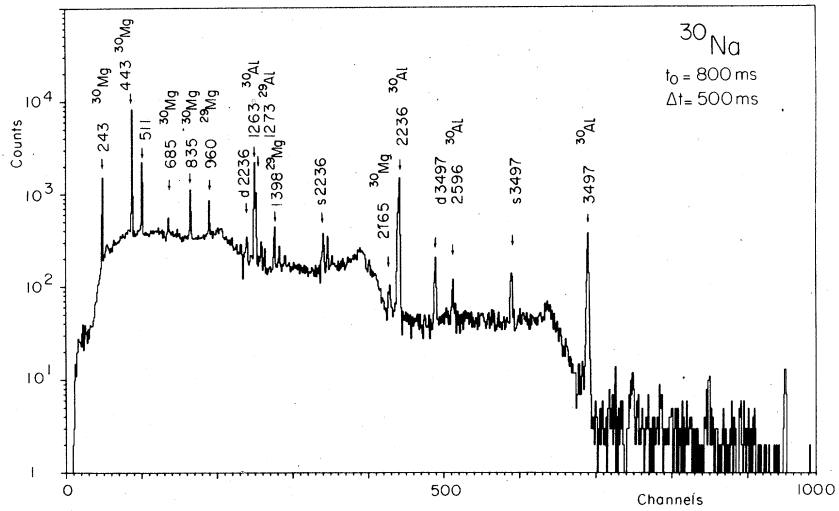

FIG. 7. Energy spectrum of the γ rays observed in the β decay of ^{30}Na, with timing conditions which favor the observation of the γ activities from the daughter nuclei (see Fig. 4).

results for ^{48}K, ^{49}K, and ^{50}K, obtained during the same five-day experiment, were reported elsewhere.[6]

II. EXPERIMENTAL METHOD

Neutron-rich isotopes of light nuclei are produced in the fragmentation of a 3 g/cm^2 U target by 24 GeV protons from the CERN synchrotron. They recoil out of the U target and are thermalized in graphite. Alkali elements selectively diffuse out of the heated material in a short time. Typically 50% of the Na atoms diffuse out within 100 ms. They are ionized through surface ionization on a rhenium foil which enhances the Z selectivity of the process and are analyzed in a mass spectrometer. Hence, only isotopes of a given Z and A are collected on an aluminum foil (see, e.g., Ref. 1), at the end of the beam transport line (Fig. 1).

However, not only Na but, because of their moderate ionization potential a small fraction of Al atoms can be ionized and analyzed. Since the dif-

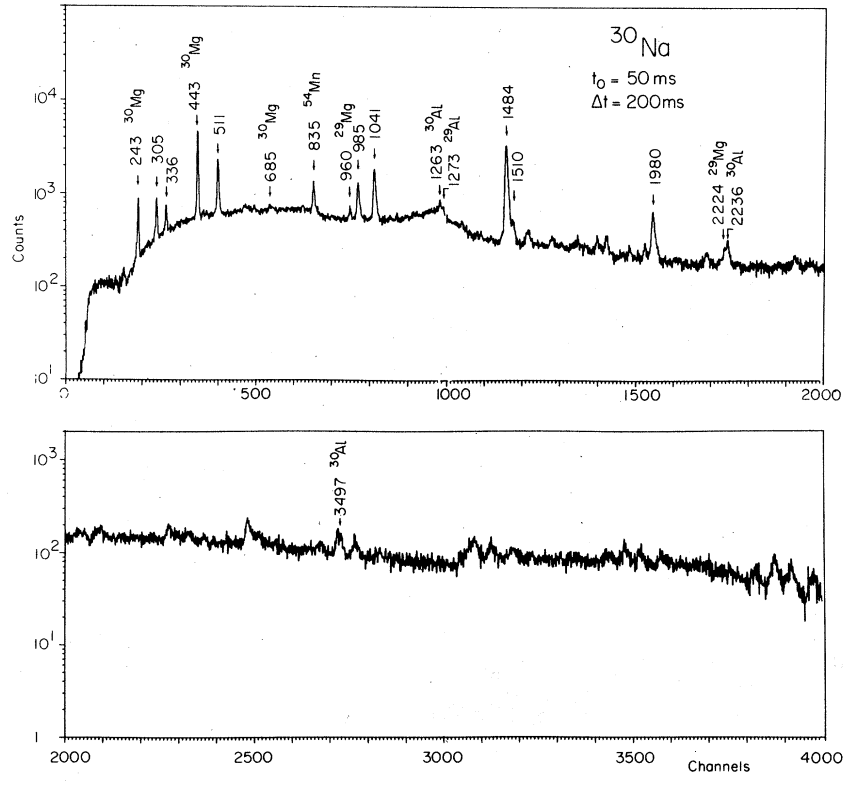

FIG. 8. Energy spectrum of the γ rays observed in the β decay of ^{30}Na (see Fig. 4).

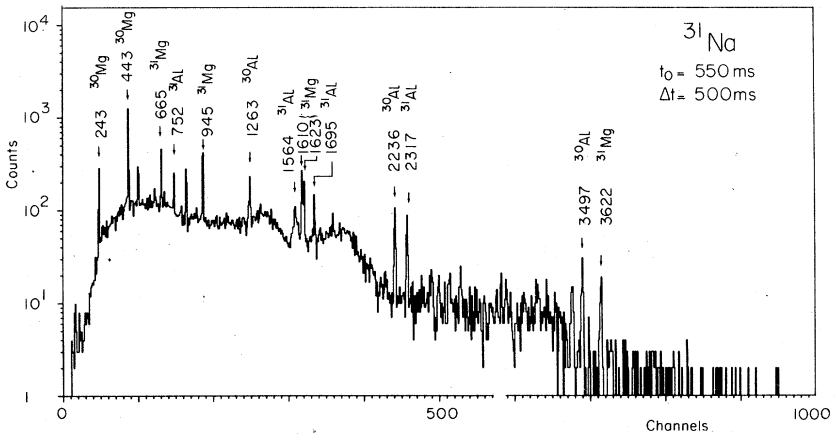

FIG. 9. Energy spectrum of the γ rays observed in the β decay of ^{31}Na, with timing conditions which favor the observation of the γ activities from the daughter nuclei (see Fig. 4).

fusion time of Al atoms out of the heated graphite is long (several tens of seconds, typically), only Al isotopes with longer half-lives can be observed, i.e., $^{27\text{-}29}$Al. In order to eliminate this Al contribution, use is made of the time structure of the CERN proton synchrotron which accelerates 10^{13} protons in a 2.1 μs burst every 2.5 s. An electrostatic deflector located on the ion beam transport line admits ions to the counting area during adjustable periods of time after the beam burst, and remains closed during the rest of the cycle.

The production cross section varies from more than 200 μb for ^{28}Na down to 500 nb for ^{32}Na. The overall efficiency of the spectrometer is of the order of 10%. For $A \geq 28$, the half-lives are shorter than 60 ms so that a part of the produced nuclei decay before diffusing out of the target. The resulting rate of collection is presented in Fig. 2.

The Al foil on which the selected ions are collected is surrounded by a thin plastic scintillator and two Ge(Li) detectors. Maximum geometrical efficiency is obtained in the compact arrangement represented in Fig. 3. The U-shaped plastic scintillator sustains a 2π solid angle. It is only 1 mm thick, having a very small efficiency for γ rays but correctly detecting β particles.

The neutron background in the counting area is limited by use of a massive shielding of 1.2 m of

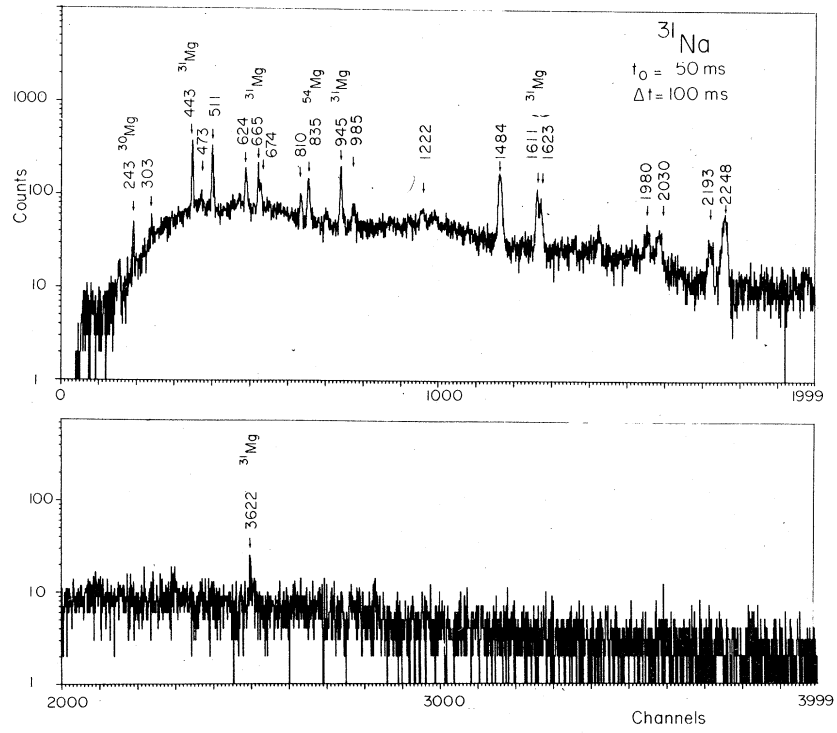

FIG. 10. Energy spectrum of the γ rays observed in the β decay of ^{31}Na (see Fig. 4).

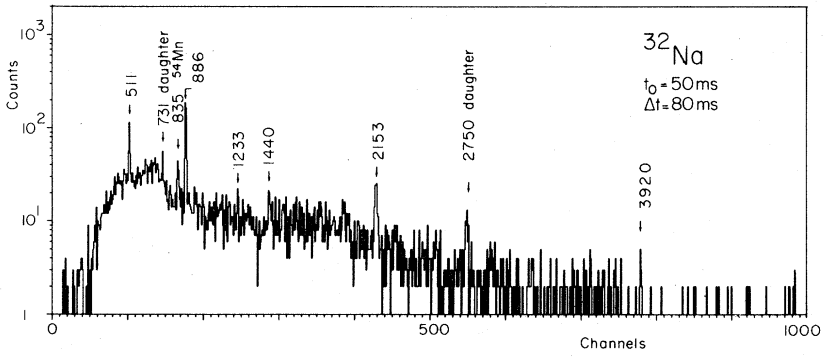

FIG. 11. Energy spectrum of the γ rays observed in the β decay of ^{32}Na (see Fig. 4). Different timing conditions allowed the observation of other γ rays listed in Tables X and XI.

iron and 3.2 m of concrete (Fig. 1). The flux of fast neutrons is reduced by one order of magnitude from the level observed in the previous experiment,[5] in spite of the higher intensity of the proton beam. This allows for the use of Ge(Li) instead of NaI detectors. However, the background still remains high enough to deteriorate the energy resolution. Therefore detectors of mediocre quality, with a typical 4 keV resolution are used, and the practical energy resolution often grows even worse in the conditions of the experiment. Furthermore, the high-energy charged particle background at the time of each beam burst is so high that the Ge(Li) preamplifier is saturated for 40 ms afterwards. This is particularly detrimental to the study of short-lived isotopes.

The purpose of the experiment is to measure the energy spectrum of the γ rays associated with the β decay of neutron-rich Na isotopes. Four successive γ energy spectra from the more efficient (15%) of the two Ge(Li) detectors are measured in between beam bursts. The half-lives of the β active nuclei are deduced from the decrease of their characteristic γ activities.

For some isotopes, $\beta\gamma\gamma$ coincidences involving photopeak events in the two Ge(Li) detectors are observed. In spite of the very low statistics, useful information can be derived in a few cases, as discussed below. A detailed account of experimental method and procedures is given elsewhere.[7]

III. EXPERIMENTAL RESULTS AND ANALYSIS

A. γ-ray energy spectra

Figures 4 to 11 show typical energy spectra of the γ activities collected after each beam burst, for different masses of the analyzed Na isotope. The time parameters, i.e., the delay after the beam burst before counting is started and the duration of the measurement, are set to ensure maximal efficiency for the observation of the isotope under consideration. In the case of mass 31 for instance, shorter (Fig. 10) or longer (Fig. 9) times enhance the observation of the parent ^{31}Na or daughter ^{31}Mg γ activities, respectively.

The energies of the γ rays are listed in Tables I to XI. The somewhat large uncertainties mainly reflect the poor energy resolution of the Ge(Li) detector, as discussed above.

B. Radioactive half-lives

The half-lives of the Na isotopes up to ^{33}Na have already been determined.[5] Figure 12 shows the

TABLE I. Energy and intensity of the γ activities from the β decay of ^{27}Na.

E_γ (keV)	$E_i \rightarrow E_f$ (MeV)	I_γ (%) this work	I_γ (%)[a]	I_γ (%)[b]
955.3 ± 0.5[c]	1.94 → 0.98	1.0 ± 0.15	<2.5	
984.6 ± 0.2[c]	0.98 → 0	86 ± 2	86.0 ± 2.9	117 ± 25
1169.2 ± 0.8[c]	3.11 → 1.94	0.65 ± 0.1	<2.9	
1698.3 ± 0.2[c]	1.70 → 0	13 ± 2	14.0 ± 2.3	14 ± 3
1939.9 ± 0.3[c]	1.94 → 0	0.65 ± 0.15	<2.7	
2443 ± 2[d]	3.43 → 0.98	0.45 ± 0.1		
2505.4 ± 2.2[c]	3.49 → 0.98	0.4 ± 0.1		
3476.1 ± 0.5[c]	3.48 → 0	0.6 ± 0.2	<2.0	
4005.6 ± 4.0[d]	4.99 → 0.98	0.6 ± 0.2		

[a] See Ref. 10.
[b] See Ref. 5.
[c] Derived from the excitation energies of the initial and final levels, as given in Ref. 11.
[d] From this work.

TABLE II. Energy and intensity of the γ activities from the β decay of ^{28}Na.

E_γ (keV)[b]	$E_i \rightarrow E_f$ (MeV)	I_γ (%) this work	I_γ (%)[a]	E_γ (keV)[b]	$E_i \rightarrow E_f$ (MeV)	I_γ (%) this work
1473.5 ± 0.5	1.47 → 0	37 ± 5	30 ± 5	3083.8 ± 0.9	4.56 → 1.47	5 ± 1
2389.2 ± 0.6	3.86 → 1.47	21 ± 3	16 ± 3	3404.6 ± 0.9	4.88 → 1.47	<0.8

[a] See Ref. 5.
[b] Derived from the excitation energies of the initial and final levels, as given in Ref. 11.

TABLE III. Energy and intensity of the γ activities from the β decay of ^{29}Mg.

E_γ (keV)	$E_i \rightarrow E_f$ (MeV)	I_γ (%) this work	I_γ (%)[c]	I_γ (%)[a] relative
960.3 ± 0.4[a]	3.18 → 2.22	15 ± 2	19 ± 7	52 ± 18
1307.5 ± 0.6[b]	3.06 → 1.75	5 ± 1	<5	<14
1397.7 ± 0.4[a]	1.40 → 0	15.5 ± 2.0	23^{+11}_{-7}	64^{+30}_{-20}
1429.9 ± 0.6[b]	3.18 → 1.75	6.5 ± 1.0	12 ± 6	34 ± 17
1753.8 ± 0.4[a]	1.75 → 0	8.0 ± 1.5	8 ± 2	22 ± 5
2223.7 ± 0.4[a]	2.22 → 0	36 ± 5	36	100 ± 6
2865.7 ± 0.6[b]	2.87 → 0	6.0 ± 1.5	4 ± 1	11.3 ± 2.4

[a] See Ref. 12.
[b] Deduced from the excitation energies of the initial and final levels, as given in Ref. 11.
[c] See Ref. 12, normalized to our value, 36%, for the 2223.7 keV γ ray.

TABLE IV. Energy and intensity of the γ activities from the β decay of ^{29}Na. These γ energies cannot be correlated with the excitation energies of ^{29}Mg levels reported in Ref. 13.

E_γ (keV)	I_γ (%) this work	I_γ (%)[a]	E_γ (keV)	I_γ (%) this work	I_γ (%)[a]
603 ± 3	0.3 ± 0.1		1638.4 ± 1.2	2.5 ± 0.5	
701 ± 3	0.40 ± 0.15		2049.1 ± 1.3	1.5 ± 0.3	4.5 ± 2.0
1040.7 ± 1.2	0.9 ± 0.2		2135 ± 3	0.95 ± 0.35	
1473.5 ± 0.5[b]	4.3 ± 0.8	7 ± 2	2559.8 ± 1.3	12.5	12.5 ± 2.0
1539.4 ± 1.2	1.5 ± 0.3		3166.9 ± 1.6	1.0 ± 0.3	3.0 ± 1.5
1586.4 ± 1.2	2.5 ± 0.5		3225.3 ± 1.6	1.0 ± 0.3	

[a] See Ref. 5.
[b] Corresponds to a 1.47 → 0 MeV transition in ^{28}Mg.

TABLE V. Energy and intensity of the γ activities from the β decay of ^{30}Mg.

E_γ (keV)	$E_i \rightarrow E_f$ (MeV)	I_γ (%) this work	E_γ (keV)	$E_i \rightarrow E_f$ (MeV)	I_γ (%) this work
242.9 ± 0.7	0.25 → 0	73.5 ± 12	684.6 ± 1.3	0.69 → 0	3.5 ± 0.6
443.2 ± 0.7	0.69 → 0.25	81 ± 16	2165.0 ± 1.6		3.0 ± 0.5

TABLE VI. Energy and intensity of the γ activities from the β decay of ^{30}Na.

E_γ (keV)	I_γ (%) this work	E_γ (keV)	I_γ (%) this work
304.6 ± 1.0	3 ± 0.5	1484.2 ± 1.0	74 ± 4
336.3 ± 1.0	2.0 ± 0.3	1510.7 ± 1.5	0.4 ± 0.1
985.4 ± 1.0	12.0 ± 1.5	1979.8 ± 1.0	15 ± 1.5
1041.2 ± 1.0[a]	22 ± 2		

[a] Corresponds to a 1.04 → 0 MeV transition in ^{29}Mg.

TABLE VII. Energy and intensity of the γ activities from the β decay of ^{31}Al.

E_γ (keV)[a]	$E_i \rightarrow E_f$ (MeV)	I_γ (%) this work	I_γ (%)[a] relative	E_γ (keV)[a]	$E_i \rightarrow E_f$ (MeV)	I_γ (%) this work	I_γ (%)[a] relative
621.81 ± 0.30	2.32 → 1.69	3.0 ± 1.0	9.94 ± 0.65				
752.23 ± 0.30	0.75 → 0	7 ± 2	18.5 ± 0.8	1694.73 ± 0.30	1.69 → 0	10.5 ± 3.0	58.9 ± 1.6
1564.49 ± 0.30	2.32 → 0.75	6.2 ± 2.0	17.3 ± 1.6	2316.64 ± 0.40	2.32 → 0	17 ± 5	72.8 ± 1.8

[a] See Ref. 14.

TABLE VIII. Energy and intensity of the γ activities from the β decay of ^{31}Mg.

E_γ (keV)	I_γ relative (%) this work	I_γ absolute (%) this work	E_γ (keV)	I_γ relative (%) this work	I_γ absolute (%) this work
665.3 ± 1.5	47 ± 10	12.2 ± 3.6			
945.3 ± 1.5	100	26 ± 8	1623.2 ± 1.5	54.7 ± 12.0	14.2 ± 4.0
1610.8 ± 1.5	81.7 ± 17.0	21.3 ± 6.0	3622 ± 3	26.7 ± 9.0	6.9 ± 2.0

TABLE IX. Energy and intensity of the γ activities from the β decay of ^{31}Na.

E_γ (keV)	I_γ relative (%)	E_γ (keV)	I_γ relative (%)
303 ± 1[a]	3.9 ± 1.2	1222 ± 2	13 ± 4
372.3 ± 1.0	2.9 ± 1.4	1259 ± 2	4.5 ± 2.2
473 ± 1	8.2 ± 2.5	1484.2 ± 1.0[a]	100
623.7 ± 1.0	37.5 ± 4.2	1979.8 ± 1.0[a]	11.2 ± 5.5
673.8 ± 1.5	23.6 ± 3.2	2030.5 ± 2.5	12 ± 4
809.8 ± 1.5	25.5 ± 4.2	2192.8 ± 2.5	17 ± 5
985.4 ± 1.0[a]	12.6 ± 3.8	2247.6 ± 2.5	58 ± 6

[a] Corresponds to transitions in ^{30}Mg (see Table VI).

TABLE X. Energy and intensity of γ activities from the β decay of descendants of ^{32}Na, ^{32}Mg and/or ^{32}Al (see text).

E_γ (keV)	I_γ relative (%)	E_γ (keV)	I_γ relative (%)
422 ± 2	21.6 ± 6.7	1939 ± 4	52.7 ± 20
731 ± 2	36.0 ± 15	2750 ± 5	100

TABLE XI. Energy and intensity of the γ activities from the β decay of ^{32}Na.

E_γ (keV)	I_γ absolute (%)	E_γ (keV)	I_γ absolute (%)
885.7 ± 2.0	80 ± 8	2153 ± 5	48 ± 10
1233 ± 4	6 ± 3	2556 ± 5	12.5 ± 6.0
1440 ± 4	7 ± 3	3920 ± 5	10.5 ± 5.0
1970 ± 5	11 ± 5		

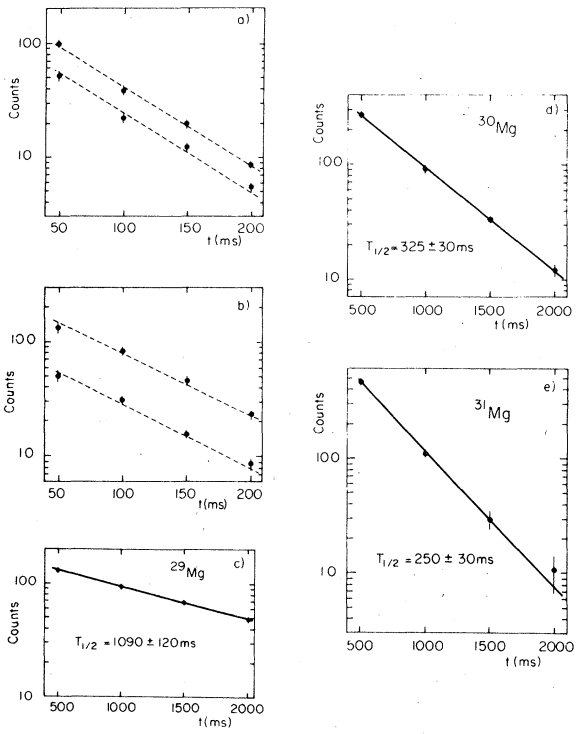

FIG. 12. Time dependence of: (a) the 1473.5 and 1586.3 keV γ activities from ^{29}Na; (b) the 1484.2 and 1041.2 keV γ activities from ^{30}Na; (c) the sum of the 960.3 and 2223.8 keV γ activities from ^{29}Mg; (d) the 443.2 keV γ activity from ^{30}Mg; (e) the sum of the 665.3 and 945.3 keV γ activities from ^{31}Mg. In (a) and (b), the dashed lines correspond to the known (Ref. 5) half-lives of ^{29}Na and ^{30}Na. In (c), (d), and (e), the full lines are fitted to the time dependence and determine the half-lives of ^{29}Mg, ^{30}Mg, and ^{31}Mg as 1090 ±120 ms, 325 ± 30 ms, and 250 ± 30 ms, respectively.

TABLE XII. Half-lives of Mg isotopes.

Isotope	This work	Previous work Ref. 5	Previous work Ref. 12
^{29}Mg	1090 ± 120	1470 ± 90	1200 ± 130
^{30}Mg	325 ± 30	1200 ± 500	
^{31}Mg	250 ± 30		

decrease with time of some of the γ activities observed in the present experiment. This decrease is correctly fitted by the known half-lives of the Na isotopes, which establishes that those γ activities are due to the β decay of Na isotopes.

The half-lives of the Mg and Al isotopes were known up to ^{30}Mg and ^{31}Al (see Table XII). In the present work, some γ activities, with longer half-lives than the Na parent and with energies which often can be assigned to transitions between energy levels of the Al descendant, are assigned to ^{30}Mg and ^{31}Mg. Their time dependence yields the half-life of those isotopes (Fig. 12). Table XII summarizes the results. The values obtained in the previous experiment[5] for ^{29}Mg and ^{30}Mg are larger than those from this work. They were derived from an analysis of the time dependence of the β activity. The contribution of the Na decay was subtracted and the remaining decrease was supposed to be due to the Mg decay. However, the contribution of the Al decay was not taken into account. It is suggested that this causes the systematic differences seen in Table XII and that the present values free from such a systematic error, are to be preferred.

For the decendants of ^{32}Na, several γ activities are observed to decay with an apparent half-life

TABLE XIII. Methods used to derive absolute values of the intensities of γ activities.

A	Isotope	Calibration method
27	Na	1) Assumption: $\sum I_\gamma(\rightarrow \text{g.s.}) = 100\%$ 2) The measured ^{27}Mg activity is used to calculate the number of parent ^{27}Na nuclei collected.
28	Na	The measured ^{28}Al activity is used to calculate the number of ^{28}Na nuclei collected.
29	Mg	The measured ^{29}Al activity is used to calculate the number of parent ^{29}Mg nuclei formed.
	Na	Assumption: The $E_\gamma = 2559.8$ keV activity has $I_\gamma = 12.5\%$ (see Ref. 5).
30	Mg	The measured ^{30}Al activity is used to calculate the number of parent ^{30}Mg nuclei formed.
	Na	Assumption: The $E_\gamma = 1484.2$ keV is the $2^+ \rightarrow 0^+$ transition in ^{30}Mg and has $I_\gamma = (100 - P_n)\%$.
31	Al and Mg	The measured ^{30}Al activity is used to calculate the number N of ^{30}Mg nuclei formed. From the P_n value of ^{31}Na (taken from Ref. 5) the number of ^{31}Mg is deduced from N; hence the number of daughter ^{31}Al nuclei is obtained.
32	Na	Assumption: The $E_\gamma = 885.7$ keV is the $2^+ \rightarrow 0^+$ transition in ^{32}Mg and has $I_\gamma = (100 - P_n)\%$.

TABLE XIV. Delayed-neutron branching ratios.

Isotope	P_n (%) this work	P_n (%)[a] (Ref. 5)
^{27}Na		0.08 ± 0.03
^{28}Na		0.58 ± 0.12
^{29}Na	21 ± 4	15.1 ± 1.8
^{30}Na	26 ± 4	33.1 ± 3.8
^{31}Na		30 ± 8
^{32}Na	20 ± 8	

ranging between 50 and 200 ms. However, because of the poor statistics (Fig. 11) no definite assignment is proposed.

C. γ intensities

In the earlier experiment,[5] the I_γ intensities were derived from the ratio of the measured γ and β activities. Here, a different method is used. I_γ is deduced from the ratio of two γ activities, the γ ray of interest and a known γ ray from a descendant, taken as a measure of the number of decaying Na isotopes. The analysis takes into account the time parameters of the measurement and the possible losses of activity in the A chain due to delayed neutron emission.

For shorter half-lives, i.e., heavier Na isotopes, that method cannot be used. This is due to the long delay between the beam burst and the beginning of the measurement, of the order of 40 ms as discussed in Sec. II. Since the time dependence of the Na yield from the source is not accurately known, the γ activity at the time of the measurement cannot be precisely related to the number of Na ions actually collected. Alternative ways are used to obtain absolute values of I_γ. For instance, for the β decay of ^{29}Na, the I_γ value (12.5%) previously measured[5] for the 2559 keV activity is taken as a normalization for the other γ rays.

As for the even ^{30}Na and ^{32}Na isotopes, it is assumed that all the β transitions that do not feed either the ground or a neutron-unstable level in ^{30}Mg and ^{32}Mg eventually give rise to a γ transition between the first 2^+ excited state and the ground state. That dominant γ activity is therefore assigned $I_\gamma = (100 - P_n)\%$ if there is no β branching to the Mg ground state.

That feature is generally observed in the known β-decay schemes of odd-odd nuclei. For ^{28}Na, which has $J = 1$,[8] there is a large β branch to the ^{28}Mg ground state, as observed previously[5] and confirmed below, but the remainder of the β strength indeed yields the $2^+ \rightarrow 0^+ \gamma$ transition. Since the spin of ^{30}Na is $J = 2$,[8] there is no allowed β transition to the ^{30}Mg ground state and the most abundant γ ray, at 1484 keV, is assigned to the $2^+ \rightarrow 0^+$ transition in ^{30}Mg with $I_\gamma = (100 - P_n)\%$.

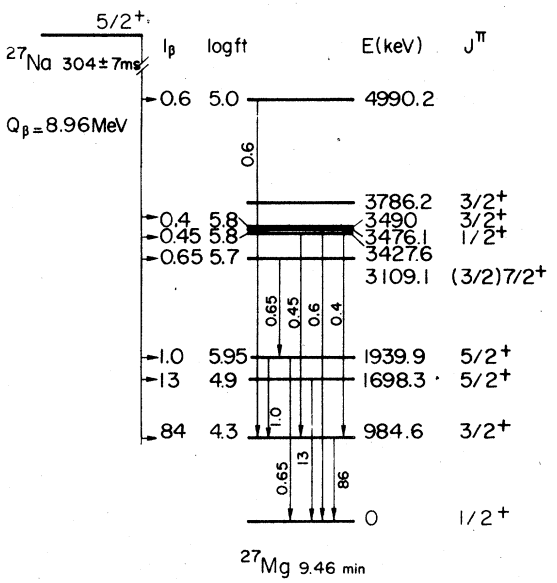

FIG. 13. Decay scheme of ^{27}Na. The energies and J^π values of the ^{27}Mg levels are taken from Refs. 11, 15, 16. Although a weak γ line is emitted by the 3476.1 keV level, no β transition to this state is indicated since the corresponding logft of 5.5 would be incompatible with its forbidden $\frac{5}{2}^+ \rightarrow \frac{1}{2}^+$ character. It is assumed that this level is fed by an unobserved γ ray from a higher level.

TABLE XV. Delayed neutron branching to excited states of the daughter nucleus.

Precursor	Daughter	Total P_n (%) (this work)	Total P_n (%) (previous work) (Ref. 5)	γ transition in the daughter nucleus E_γ (keV)	I_γ (%)
^{29}Na	^{28}Mg	21 ± 4	15.1 ± 1.8	1473.5 ± 0.5	4.3 ± 0.8
^{30}Na	^{29}Mg	26 ± 4	33.1 ± 3.8	1041.2 ± 1.0	22 ± 2
^{31}Na	^{30}Mg		30 ± 8	985.4 ± 1.0	
				1484.2 ± 1.0	
				1979.8 ± 1.0	

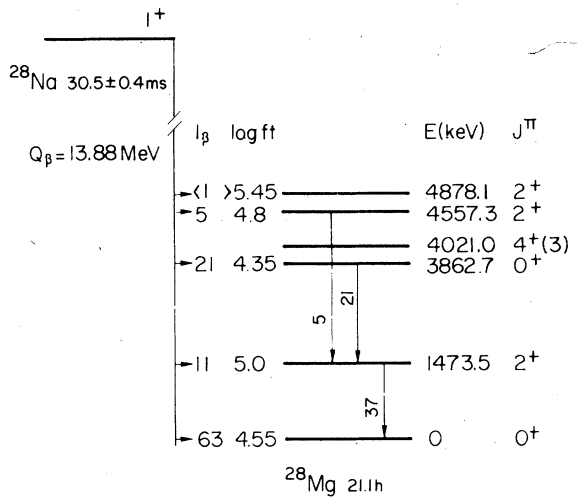

FIG. 14. Decay scheme of ^{28}Na. The energies and J^π values of the ^{28}Mg states are taken from Ref. 17.

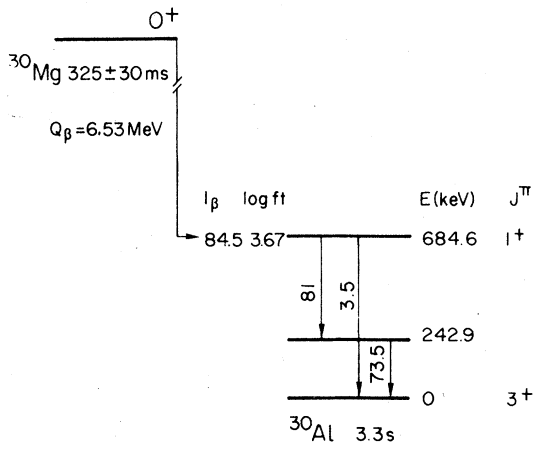

FIG. 16. Decay scheme of ^{30}Mg. The 2165 keV γ activity corresponds to a transition between unknown ^{30}Al levels. Its weak intensity (3.0%) would hardly affect the I_β and logft values.

Although the spin of ^{32}Na is unknown, the same situation is assumed to occur and again the dominant γ ray at 886 keV is assigned to the $2^+ \rightarrow 0^+$ transition with $I_\gamma = (100 - P_n)\%$. One argument for the absence of a β transition to the ^{32}Mg ground state is the likely negative parity of ^{32}Na ($Z=11$, $N=21$).

The values of P_n are either taken from Ref. 5 or remeasured as described in the next section. Table XIII summarizes the hypotheses which underline the I_γ calculations and indicates the method used in each case. The results obtained are listed in Tables I through XI.

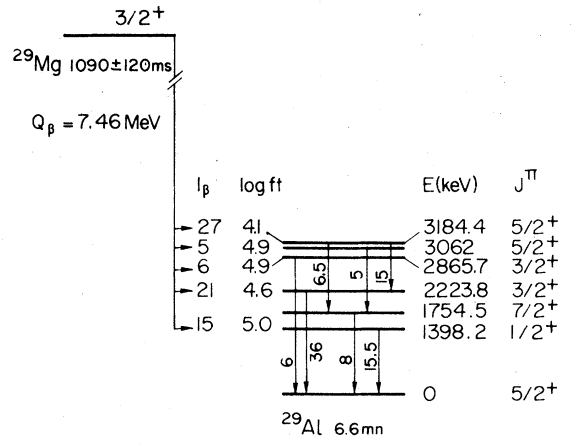

FIG. 15. Decay scheme of ^{29}Mg. The energies and J^π values are taken from Refs. 18, 12 and 11, respectively, except for the $\frac{7}{2}^+$ assignment of the 1754.5 keV level (see Ref. 19). The observation of allowed β transition to levels with $J^\pi = \frac{5}{2}^+$ restricts the $(\frac{3}{2}^+, \frac{1}{2}^+)$ J^π assignment (Ref. 12) of ^{29}Mg to $J^\pi = \frac{3}{2}^+$.

D. Delayed neutron emission

Delayed neutron emission is a general phenomenon in the β decay of neutron-rich nuclei far from stability, and it is only for practical reasons that most known delayed neutron emitters are fission fragments. In a previous experiment[5] the Na isotopes from ^{27}Na up to ^{31}Na were added to the list. We recently observed delayed neutron emission from ^{50}K.[6]

The delayed neutron branching ratios P_n are measured from the ratio of two γ activities. In the β decay of ^{A}Na, we compare a known γ activity from the β decay of $^{A-1}$Mg or $^{A-1}$Al, which is taken as a measure of the delayed neutron branching, to a γ activity from the β decay of ^{A}Mg or ^{A}Al.

This new method is independent from the one

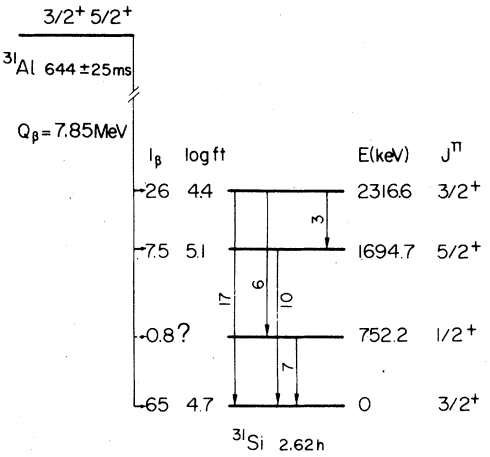

FIG. 17. Decay scheme of ^{31}Al. The energies and J^π values of the ^{31}Si levels are taken from Ref. 14.

used by Roeckl *et al.*[5] who measured P_n as the ratio between the neutron and β activities. Table XIV presents our and Roeckl's results, which are in good agreement.

In the β decay of ^{32}Na, a 945 keV γ activity from ^{31}Al is observed, which indicates that ^{32}Na, as expected, is also a delayed neutron emitter. A 20 $\pm 8\%$ P_n value is deduced from the intensity of that γ ray.

In a few cases, a γ activity is observed with the half-life of ^{A}Na and an energy which can be assigned to a transition between levels of $^{A-1}$Mg. It corresponds to a process in which the delayed neutron from an unbound state of ^{A}Mg feeds an excited state in the daughter $^{A-1}$Mg nucleus. This particular process, already reported for fission fragments (see, e.g., Ref. 9), is observed here for ^{29}Na, ^{30}Na, and ^{31}Na (Table XV).

E. Decay schemes and β branching ratios

When the level scheme of the daughter nucleus is known, γ energies and intensities alone can determine the β decay scheme. The β branching ratio to a level of the daughter nucleus is then taken as the difference between the intensities of the γ rays from and to this level. This method is used for the β decay of ^{27}Na and ^{28}Na, ^{29}Mg and ^{30}Mg, and ^{31}Al (Figs. 13 to 17).

Although the level scheme of ^{30}Mg is unknown, a partial β-decay scheme can be derived for ^{30}Na. Among the seven γ activities listed in Table VI, one, at 1041 keV, was assigned in the preceding section to a γ transition in ^{29}Mg following delayed neutron emission. Two γ rays, at 985 and 1484 keV, are found to be in coincidence. It is assumed that a 2.46 MeV level of ^{30}Mg, populated in the β decay of ^{30}Na, decays by γ emission to the 1.48 MeV first excited state which is assigned $J^{\pi}=2^{+}$, as discussed in Sec. IIIC. The resulting tentative β-decay scheme of ^{30}Na is represented in Fig. 18.

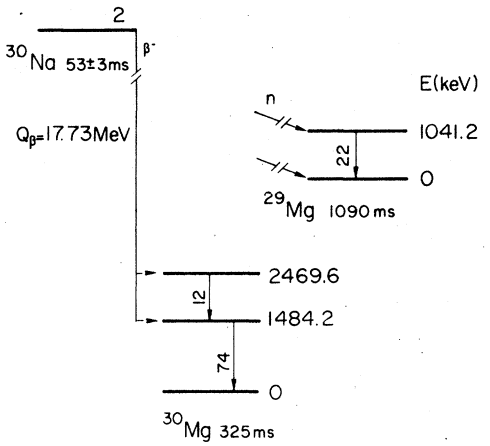

FIG. 18. Partial decay scheme of ^{30}Na. The two γ transitions in ^{30}Mg which are represented are observed in coincidence. The intense (74%) 1484 keV γ ray is assumed to correspond to the $2^{+} \rightarrow 0^{+}$ transition in ^{30}Mg. Four other γ activities from ^{30}Na (Table VI) cannot be assigned since no excited state of ^{30}Mg is known. It is to be noted that most of the delayed-neutron branch ($P_n = 26\%$, see Table XV) corresponds to the emission of neutron leaving the daughter ^{29}Mg nucleus in its 1041.2 keV ($I_\gamma = 22\%$) state.

IV. CONCLUSION

The most prominent γ rays observed in the decay of ^{30}Na and ^{32}Na have been assigned to the $2^{+} \rightarrow 0^{+}$ transition in the daughter nuclei, as discussed in Sec. IIIC. Figure 19 summarizes the resulting location of the first 2^{+} excited states of Mg isotopes. The strong decrease observed for ^{32}Mg is taken as evidence for an increased deformation of this isotope, thus providing a reasonably model free confirmation of the suggestion[1,2] of a new region of deformation starting near $N=20$ for the Na isotopes and neighboring elements.

The method used in this work has not reached the limits of its sensitivity yet. Higher efficiencies for the Ge(Li) detectors and still better shielding would result in better statistics and more accurate energy values. It would allow for an easier observation of $\gamma\gamma$ coincidences. The lower background would also make possible the measurement of γ activities a few ms after the beam burst, which is necessary to study short-lived isotopes. The β decay of ^{34}Na is certainly accessible to the method, and the location of the first 2^{+} state of ^{34}Mg is indeed of major interest since the theoretical calculations mentioned in Sec. I predict an increasing deformation of the Na isotopes with increasing N.

Furthermore, two interesting modes of decay are energetically possible for the very neutron-rich

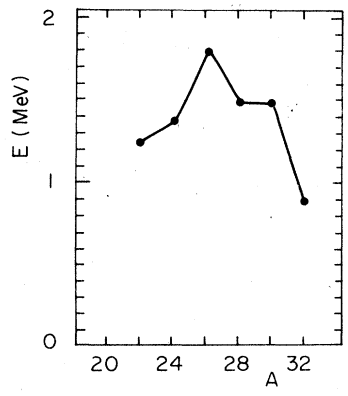

FIG. 19. Variation with A of the excitation energy of the first 2^{+} state in even-even Mg isotopes. The values for ^{30}Mg and ^{32}Mg are determined in this work.

isotopes under consideration and are within reach of the experimental method: (i) delayed two-neutron emission which could be characterized by, e.g., the γ activity of ^{28}Mg formed in the β decay of ^{30}Na; (ii) delayed α emission, generally observed for neutron-deficient isotopes, which could occur in the β decay of ^{30}Na and heavier isotopes.

ACKNOWLEDGMENTS

It is a pleasure to acknowledge the outstanding contributions of R. Fergeau, M. Jacotin, and J. F. Kepinski for many valuable instrumental developments and their assistance at CERN before and during the run. The contributions of B. Rosenbaum who developed a data acquisition buffer for the PDP 15 on-line computer, and of G. Le Scornet who wrote the corresponding program are gratefully acknowledged. We thank A. Ball, J. M. Michaud, J. Zaslavsky, and many members of the CERN Experimental Facilities Division for their assistance in setting up and maintaining the complex proton beam transport from the P.S. We are indebted to P. Constanta CERN summer student who, while participating in a companion experiment, was of great help during the run.

---

*Permanent address: Isolde Group, CERN, Geneva.
[1]C. Thibault, R. Klapisch, C. Rigaud, A. M. Poskanzer, R. Prieels, L. Lessard, and W. Reisdorf, Phys. Rev. C 12, 644 (1975).
[2]X. Campi, H. Flocard, A. K. Kerman, and S. Koonin, Nucl. Phys. A251, 193 (1975).
[3]R. K. Sheline, in Proceedings of the Third International Conference on Nuclei far from Stability, CERN Report No. 76–13 (unpublished).
[4]M. Beiner, R. J. Lombard, and D. Mas, Nucl. Phys. A249, 1 (1975).
[5]E. Roeckl, P. F. Dittner, C. Détraz, R. Klapisch, C. Thibault, and C. Rigaud, Phys. Rev. C 10, 1181 (1974).
[6]C. Détraz, D. Guillemaud, G. Huber, R. Klapisch, M. Langevin, F. Naulin, C. Thibault, L. C. Carraz, and F. Touchard, Nucl. Phys. A302, 41 (1978).
[7]D. Guillemaud, Thèse de 3ème cycle, Orsay Report No. IPNO-T-78-01, 1978 (unpublished).
[8]G. Huber, F. Touchard, S. Büttgenbach, C. Thibault, R. Klapisch, H. T. Duong, S. Liberman, J. Pinard, J. L. Vialle, P. Juncar, and P. Jacquinot, Phys. Rev. C 18, 2342 (1978).
[9]K. L. Kratz, W. Rudolph, H. Ohm, H. Franz, C. Ristori, M. Zendel, G. Herrmann, F. M. Nuh, D. R. Slaughter, A. A. Shihab-Eldin, and S. G. Prussin, in Proceedings of the Third International Conference on Nuclei far from Stability, CERN Report No. 76–13 (unpublished).
[10]D. E. Alburger, D. R. Goosman, and C. N. Davids, Phys. Rev. C 8, 1011 (1973).
[11]P. M. Endt and C. Van Der Leun, Nucl. Phys. A214 (1973).
[12]D. R. Goosman, C. N. Davids, and D. E. Alburger, Phys. Rev. C 8, 1331 (1973).
[13]D. K. Scott, B. G. Harvey, D. L. Hendrie, L. Kraus, C. F. Maguire, J. Mahoney, Y. Terrien, and K. Yagis, Phys. Rev. Lett. 33, 1343 (1974).
[14]D. R. Goosman and D. E. Alburger, Phys. Rev. C 6, 2409 (1973).
[15]F. Meurders and A. Van Der Steld, Nucl. Phys. A 230, 317 (1974).
[16]G. Costa and F. A. Beck, Nucl. Phys. A181, 132 (1972).
[17]P. Fintz, B. Rastegar, N. E. Divison, F. Hibou, G. Guillaume, and A. Gallman, Nucl. Phys. A197, 423 (1972).
[18]P. Ekström and J. Tillman, Nucl. Phys. A230, 285 (1974).
[19]F. A. Beck, T. Byrski, A. Knipper, and J. P. Vivien, Phys. Rev. C 13, 1792 (1976).